Jin et al. *Zool. Res.* 2026, 47(1): 32−40
https://doi.org/10.24272/j.issn.2095-8137.2025.118
https://cstr.cn/32248.14.zr.2025.118

ZR | Zoological Research

Article Open Access

Establishment of a transgenic protocol in *Trichoplax adhaerens*

Min-Jun Jin[1,3,#,*], Zhong-Yu Ji[1,3,#], Zi-Yi Zhao[1,3], Qiu-Yao Guo[1,3], Guo-Tao Di[1,3], Wan-Qing Li[1,3], Cheng-Tian Zhao[1,2,3,*]

[1] *Fang Zongxi Center for Marine EvoDevo*, *MoE Key Laboratory of Marine Genetics and Breeding*, *College of Marine Life Sciences*, *Ocean University of China*, *Qingdao*, *Shandong* 266003, *China*

[2] *Laboratory for Marine Biology and Biotechnology*, *Qingdao Marine Science and Technology Center*, *Qingdao*, *Shandong* 266237, *China*

[3] *Institute of Evolution & Marine Biodiversity*, *Ocean University of China*, *Qingdao*, *Shandong* 266003, *China*

ABSTRACT

Trichoplax adhaerens, one of the simplest multicellular organisms belonging to the phylum Placozoa, occupies a basal position within Metazoa and serves as a critical model for investigating early multicellular evolution. Despite its significance, the absence of functional genetic tools has limited research to comparative genomics, ultrastructural characterization, and behavioral observation. Developing methodologies such as transgenesis and gene editing would substantially expand experimental capabilities. However, the absence of sexual reproduction precludes the use of conventional approaches like single-cell microinjection. To overcome these limitations, the present study established a transgenic method for expressing exogenous genes in *T. adhaerens*. Systematic evaluation of multiple transfection techniques identified electroporation as the most effective strategy for inducing ectopic gene expression in this species. Electroporation parameters were optimized to maximize efficiency while minimizing cytotoxicity. Using this approach, robust expression of green fluorescent protein (GFP) was achieved using various promoters. Ectopic expression of the puromycin acetyltransferase (*PAC*) gene conferred increased resistance to puromycin exposure, suggesting a potential strategy for generating stable transgenic lines in the future. This work introduces a reliable framework for ectopic gene expression in *T. adhaerens*, enabling molecular and functional analyses in one of the earliest-diverging metazoan lineages.

Keywords: *Trichoplax adhaerens*; Transgenic; Electroporation; Placozoa; Basal metazoan

INTRODUCTION

Placozoans, alongside ctenophores, poriferans, and cnidarians, comprise one of the four earliest-diverging animal lineages (Schultz et al., 2023). Among these, placozoans exhibit the most reduced and morphologically simple body plan, making them an excellent model for studying the origins and evolution of multicellularity. *Trichoplax adhaerens* represents the most well-characterized placozoan species (Schierwater et al., 2021; Schulze, 1883). Despite its compact genome containing fewer than 100 megabases, *T. adhaerens* retains a large repertoire of highly conserved genes shared with vertebrates and other metazoans, including humans (Bi & Zhang, 2021; Srivastava et al., 2008).

Histological and ultrastructural analyses have identified six primary cell types in *T. adhaerens*. Motility is driven by ciliated epithelial cells on both ventral and dorsal surfaces. The ventral layer also includes scattered populations of gland cells, which secrete mucus and signaling molecules, and lipophil cells, which harbor lipid-rich granules and contribute to extracellular digestion of algae (Smith & Mayorova, 2019). Between these epithelial layers, contractile fiber cells extend filopodia that mediate contractility and phagocytosis (Mayorova et al., 2021). Dorsal epithelial cells contain shiny spheres, specialized structures implicated in predator defense (Jackson & Buss, 2009). Transcriptomic and single-cell profiling have revealed a broader cellular repertoire than previously recognized, including multiple peptidergic cell types with distinct transcriptional signatures that regulate coordinated feeding and locomotory behaviors (Najle et al., 2023; Smith et al., 2015; Varoqueaux et al., 2018).

Although substantial progress has been made in decoding the morphology, genomic architecture, and behavioral repertoire of *T. adhaerens*, functional investigations of specific genes remain severely constrained. The absence of reliable genetic manipulation tools, particularly transgenic methods,

Received: 22 June 2025; Accepted: 30 July 2025; Online: 31 July 2025

Foundation items: This work was supported by the National Natural Science Foundation of China (32125015 to C.T.Z.; 324B2023 to W.Q.L.), Laoshan Laboratory (LSKJ202203204 to C.T.Z.), and Postdoctoral Fellowship Program of CPSF (GZC20251747 to M.J.J.)

[#]Authors contributed equally to this work

*Corresponding authors, E-mail: jinminjun@ouc.edu.cn; chengtian_zhao@ouc.edu.cn

has hindered efforts to probe causal relationships between genes and phenotypes. In contrast, transgenic systems have been successfully implemented in other basal metazoans, including poriferans and cnidarians. The obligate asexual reproduction of *T. adhaerens* presents a major technical obstacle that precludes conventional germline-based transgenesis. Additionally, the presence of thousands of cells in each individual further complicates efforts to achieve efficient and uniform transgene delivery.

This study established a transgenic method for introducing and expressing exogenous genes in *T. adhaerens*. Through a comparative assessment of transfection techniques, electroporation was identified as an effective delivery platform for gene transfer. Optimization of electroporation conditions enabled sustained expression of green fluorescent protein (GFP) under the control of an endogenous β-actin promoter. These advances provide a foundational genetic toolkit for functional genomics in placozoans and open new avenues for mechanistic investigation into cell type diversification and early metazoan evolution.

MATERIALS AND METHODS

Animals

Trichoplax adhaerens was kindly provided by Professor Leo Buss (Yale University) and Dr. Carolyn L. Smith (National Institutes of Health). Cultures were maintained using the marine phytoplankton *Rhodomonas salina* as a food source. Organisms were reared in 120 mm or 180 mm glass Petri dishes filled to 80% capacity with seawater filtered through a 0.22 μm membrane and sterilized under high pressure. Following seawater addition, 5–10 mL of algal culture and 10–15 *T. adhaerens* individuals were inoculated into each dish. Cultures were incubated for 4–7 days to promote algal proliferation and were maintained at room temperature with biweekly seawater replacement (Heyland et al., 2014).

Plasmid construction

An endogenous *T. adhaerens β-actin* promoter was cloned using the following primers: forward: 5′-GCGAATTCCAAC TGCTGCCCGTTAATAAAAC-3′ and reverse: 5′-CGGGATC CATTGGATTGCAATTGATTTTC-3′. The amplified 2.18 kb fragment contained the upstream region of the *Tad56111* gene, spanning from the 3′ end of the preceding gene to the translation start site. This fragment replaced the CMV promoter in the pcDNA3.0-CMV-GFP plasmid. Distinct primer sets were used to distinguish GFP mRNA expression from non-specific amplification of the transfected DNA plasmid.

Microinjection

For microinjection, *T. adhaerens* specimens were transferred to 32 mm Petri dishes. DNA or fluorescent dextran was loaded into injection needles using a microloader. Microinjections were performed under a 5× objective using the FemtoJet system coupled with a TransferMan 4r manipulator. Each individual received approximately 50 ng of plasmid DNA. Control animals were injected with artificial seawater in equivalent volumes. After 4–6 h, 80% of the seawater was replaced, and dishes were incubated in darkness for 24 h.

Transfection by liposome, polyethylenimine (PEI), and spiky silica nanoparticle (SSN) reagents

For liposome- and PEI-mediated transfection, 3 μg of plasmid DNA was mixed with 50 μL of seawater in a 200 μL centrifuge tube. Transfection reagent, either Liposome (Hieff Trans® Liposomal Transfection Reagent, Yeasen, China) or PEI (Hieff Trans®Polyethylenimine Linear MW 40000, Yeasen, China), was then added along with an additional 50 μL of seawater. *Trichoplax adhaerens* individuals were transferred into wells of a 24-well plate prefilled with 350 μL of seawater, followed by the addition of transfection solution to reach a final volume of 500 μL. The animals were incubated for at least 24 h before further analysis. For SSN-mediated transfection, 10 μg of plasmid DNA was mixed with 50 μL of seawater, followed by the addition of 10 μL of SSN reagent. The mixture was incubated for 15 min before proceeding with transfection.

Electroporation

Animals were transferred to 35 mm Petri dishes containing artificial seawater (11 mmol/L $CaCl_2$, 10 mmol/L KCl, 40 mmol/L $MgCl_2$, 15 mmol/L $MgSO_4$, 435 mmol/L NaCl, 2.5 mmol/L $NaHCO_3$, 7 mmol/L Tris base, 13 mmol/L Tris-HCl, ddH_2O to 1 L, pH 8.2) and rinsed twice with fresh seawater. Specimens were then transferred to 1.5 mL centrifuge tubes. After removing excess seawater, electroporation buffer containing 320 μL of 0.96 mol/L mannitol (Sigma, M4125, USA) and 30 μg of plasmid DNA was added, bringing the final volume to 400 μL. The mixture was transferred to an electroporation cuvette (Bio-Rad, 165-2088, USA) and subjected to electroporation at 70 V and 1 500 μF using a Gene Pulser Xcell system (Bio-Rad, USA). Immediately following electroporation, animals were returned to Petri dishes and washed twice by replacing 80% of the medium with fresh seawater. Incubation was carried out in the dark until analysis.

Cell dissociation

For single-cell preparation, animals were transferred to 1.5 mL centrifuge tubes and rinsed to remove residual seawater. Approximately 30 μL of calcium- and magnesium-free artificial seawater (449 mmol/L NaCl, 9 mmol/L KCl, 33 mmol/L Na_2SO_4, 2.15 mmol/L $NaHCO_3$, 10 mmol/L Tris-Cl, 2.5 mmol/L EGTA, ddH_2O to 1 L, pH 8.2) was added. Specimens were pipetted to generate small fragments. Subsequently, 0.3 μL of Liberase™ DH enzyme (Roche, 551551, Switzerland) was added, and the mixture was incubated at 37°C for 15–20 min. Gentle pipetting facilitated dissociation into single cells.

Immunofluorescence assay

Animals were placed in 32 mm plastic dishes containing approximately 1 mL of seawater and flash-frozen on dry ice for 13 s. Samples were then prechilled in −80°C methanol for 30 s and stored at −80°C overnight. The following day, samples were washed in a 1:1 mixture of PBST (1× phosphate-buffered saline (PBS), 0.1% Tween-20) and methanol for 30 min, followed by three PBST washes (each 30 min). Blocking was performed for 1 h at room temperature using a buffer containing 3% goat serum, 2% horse serum, and 1% bovine serum albumin (BSA). Samples were incubated overnight at 4°C with a GFP primary antibody (1:500; Abcam, ab290, UK). After washing, samples were incubated with a secondary goat anti-rabbit IgG antibody (1:500) following standard protocols. Confocal imaging was performed on a Zeiss LSM900 microscope (Germany).

Gene expression analysis

Groups of at least 20 animals were washed with clean seawater and transferred to 1.5 mL centrifuge tubes. After brief centrifugation, residual seawater was removed. Total

RNA was extracted using the RNA Isolation Kit-BOX2 (Vazyme, China), and reverse-transcribed into cDNA using the HiScript III 1st Strand cDNA Synthesis Kit (Vazyme, China). Reverse transcription-quantitative polymerase chain reaction(RT-PCR) amplification was conducted using 2× Taq Pro Master Mix (Vazyme, China) according to the manufacturer's instructions.

Puromycin treatment

At 24 h post-electroporation, approximately 30 animals were transferred to 35 mm Petri dishes containing sterilized seawater. Puromycin was applied daily at 3 μg/mL for the first 3 days, with medium replaced daily with freshly prepared puromycin at the same concentration and an appropriate amount of algae added as a food source. On day 4, 1 μg/mL puromycin was administered for 24 h (with algae), followed by 4 μg/mL on day 5 (also with algae). This two-day alternating cycle of 1 μg/mL and 4 μg/mL treatments was continued from day 6 onward.

RNA sequencing (RNA-seq) analysis

Single-cell RNA-seq (scRNA-seq) data were obtained from Figshare (10.6084/m9.figshare.26798683). Data were processed in R v.4.3.2 and Seurat v.5.0.1 was used for cell clustering with the parameters dims=1:10 and resolution=0.5. Clustering distances were visualized using the Uniform Manifold Approximation and Projection (UMAP). Marker genes were identified using the FindAllMarkers function and used for annotating clusters. RNA-seq read quality was assessed using Fqtrim v.0.9.7, followed by alignment to the reference genome with STAR v.2.7.6a. Read counts were reported using FeatureCounts, and transcripts per million (TPM) were calculated using R.

Statistical analysis

GraphPad Prism 9 was used for all statistical analyses. For normally distributed data, either unpaired two-tailed *t*-tests or one-way analysis of variance (ANOVA) was applied. Significance levels were indicated accordingly, with ns denoting non-significance. Graphs were generated using Prism 9, and all data are presented as mean±standard deviation (SD). All experiments were independently repeated at least three times.

RESULTS

Assessment of GFP transfection efficiency in *T. adhaerens*

Phylogenomic reconstructions place Placozoa as a sister lineage to Cnidaria and Bilateria, diverging after Porifera but preceding the emergence of complex tissue organization (Figure 1A) (Schultz et al., 2023). Morphologically, *T. adhaerens* exhibits a flattened, disk-shaped body, approximately 1–2 mm in diameter and 25 μm in thickness. Under laboratory conditions, reproduction occurs primarily via binary fission (Figure 1B).

Due to the absence of gametogenesis, initial efforts focused on evaluating the feasibility of microinjection. Considering the trilaminar body structure, fluorescent particles were introduced into the intercellular space between the dorsal and ventral layers to assess diffusion throughout the entire body. Three molecular weight variants of fluorescent dextran—10 kDa rhodamine B isothiocyanate and 70 kDa and 2 000 kDa fluorescein isothiocyanate—were injected into the animals. At 1 h post-injection, robust intracellular fluorescence was detected throughout the body (Supplementary Figure S1A). Dissociation and single-cell imaging at 6 h post-injection revealed internalized fluorescence within individual cells, indicating successful uptake (Supplementary Figure S1A). Quantitative analysis showed fluorescent cell proportions of 34.9% (FD2000), 38.2% (rhodamine B), and 40.5% (FD70) (Supplementary Figure S1B). Unexpectedly, some fluorescent cells were also present in the control group. Autofluorescence analysis revealed a broad-spectrum signal in both fixed and live specimens (Supplementary Figure S2A, B), with high-resolution imaging localizing the signal to pigment granules in fiber cells (Supplementary Figure S2C) (Smith & Reese, 2016).

Subsequent microinjection of a GFP expression construct under the control of the CMV promoter yielded minimal fluorescence at 24 h post-injection (Figure 1C). Enzymatic dissociation followed by single-cell imaging indicated GFP-positive signals in only 17.18% of cells—marginally above the control background of 11.74% (Figure 1D)—suggesting inefficient cellular uptake of plasmid DNA through extracellular plasmid injection.

To identify more effective delivery methods, several transfection approaches were tested. Liposome- and PEI-mediated transfections yielded fluorescent cell frequencies of 21.8% and 22.7%, respectively (Figure 1C, D). A nanoparticle-based strategy using SSNs (Fu et al., 2022) achieved a slightly higher rate of 23.8% (Figure 1C, D). Among all methods evaluated, electroporation yielded the highest GFP-positive cell percentage, reaching 27.6% (Figure 1C, D) and exhibited enhanced fluorescence intensity at the organismal and cellular levels (Figure 1C). Quantitative analysis further showed a marked increase in GFP signal intensity per cell following electroporation (Supplementary Figure S3A). Transgene expression was independently validated by RT-PCR, which confirmed the presence of GFP transcripts (Figure 1E). To distinguish genuine GFP expression from intrinsic autofluorescence, a laser bleaching assay was performed. Autofluorescent signals remained stable under bleaching conditions, whereas GFP-derived signals were rapidly quenched, demonstrating authentic reporter expression (Figure 1F). Consistent with this distinction, GFP fluorescence displayed a diffuse intracellular distribution, whereas autofluorescence appeared as punctate granules confined within cells (Figure 1F).

Optimization of electroporation procedure in *T. adhaerens*

To improve transfection efficiency, electroporation parameters were systematically optimized by varying voltage and capacitance. Eleven distinct electroporation conditions were tested and evaluated based on tissue damage, survival rate, and the proportion of GFP-positive cells at 24 h post-treatment. Mannitol was included in the electroporation buffer to increase transfection efficiency (Figure 2A) (Christiaen et al., 2009).

Notably, electroporation induced visible lesions in many animals, including epithelial disruption and surface perforations (Figure 2B; Supplementary Figure S3B). In most cases, these injuries resolved spontaneously within 12 h (Supplementary Figure S3C). However, higher voltage and capacitance combinations increased the severity of electroporation-induced damage and were accompanied by a gradual decline in survival (Figure 2C). In contrast, GFP-

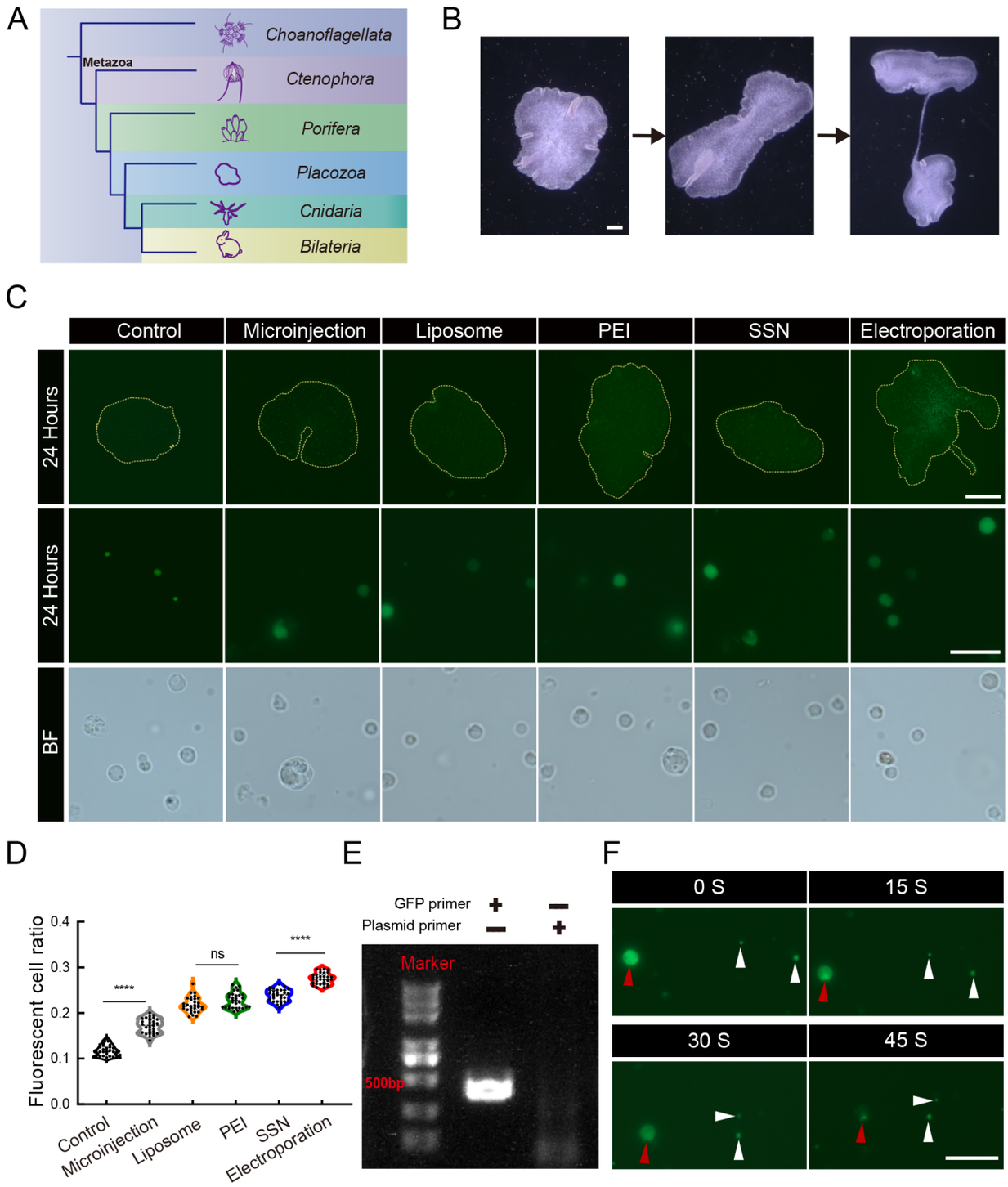

Figure 1 Evaluation of transfection efficiency in *Trichoplax adhaerens*

A: Cladogram depicting phylogenetic relationships among Bilateria and four basal metazoan lineages. B: Microscopy images showing asexual fission in *T. adhaerens*. C: Comparison of fluorescence across different plasmid transfection methods. Dotted lines outline organismal boundaries. Bright-field (BF) and corresponding fluorescence images of dissociated single cells are shown below. D: Quantification of fluorescent cell percentages under different transfection methods (autofluorescent cells were included in the analysis). Data are presented as mean±SD (n=3 independent experiments). Statistical analysis was performed using unpaired Mann-Whitney tests. E: Detection of GFP expression at 24 h post-electroporation. Negative controls used plasmid-specific primer pairs to exclude amplification from residual plasmid DNA. F: Time-lapse images showing fluorescence bleaching in a GFP-expressing cell (red arrow). White arrows indicate small autofluorescent particles that retain fluorescence during laser bleaching. S, seconds. Scale bars: 100 μm in B; 200 μm (top) and 20 μm (bottom) in C; 20 μm in F. ns: Not significant; *: P<0.05; **: P<0.01; ***: P<0.001; ****: P<0.0001.

positive cell percentages increased progressively with increasing voltage and capacitance, peaking at 37.2% and 37.5% under 70 V–2 000 μF and 70 V–1 500 μF, respectively. However, exposure to 75 V–1 500 μF caused extensive damage and reduced transfection efficiency, as reflected by a lower fluorescent cell ratio (Figure 2D). Given the lower

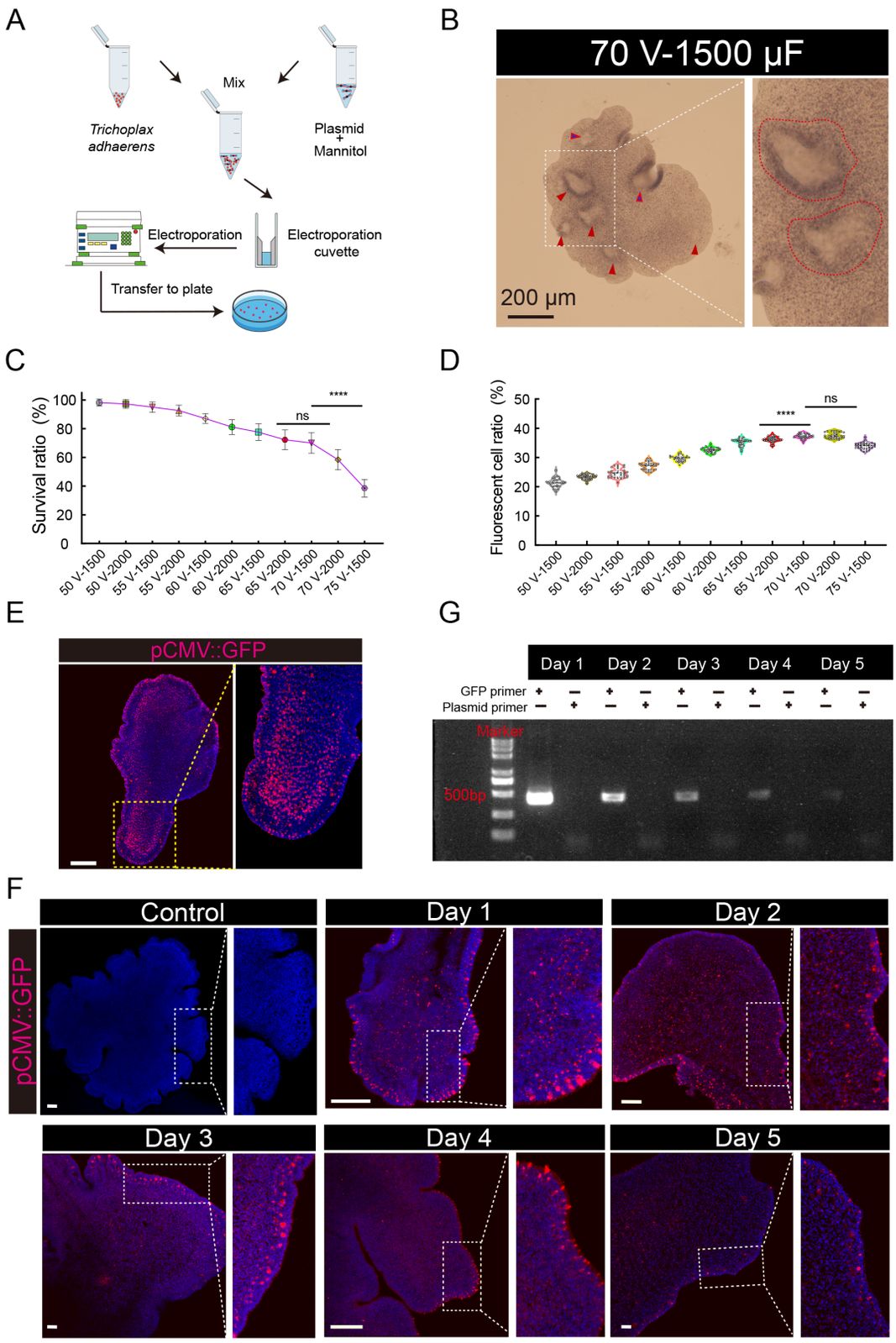

Figure 2 Optimization of electroporation parameters and validation of transgene expression in *Trichoplax adhaerens*

A: Schematic overview of the electroporation workflow in *T. adhaerens*. B: External morphology of animals post-electroporation. Red arrows indicate electropore formation sites; red dotted lines indicate large membrane discontinuities associated with epithelial layer disruption loss. Additional conditions are shown in Supplementary Figure S3B. C: Survival ratio of animals subjected to electroporation under varying voltage and capacitance settings. D: Quantification of GFP-positive cells under different electroporation conditions. E: Immunofluorescence staining with anti-GFP antibody at 24 h post-electroporation. F: Time-course immunofluorescence imaging of GFP expression at different time points after electroporation. G: RT-PCR validation of GFP expression at various time points. Scale bars: 200 μm in B and 50 μm in E, F. Data are presented as mean±SD. Statistical analysis was performed using unpaired Mann-Whitney tests. ns: Not significant; *: P<0.05; **: P<0.01; ***: P<0.001; ****: P<0.0001.

survival rate at 70 V–2 000 μF (58%) compared to 70 V–1 500 μF (70%), 70 V–1 500 μF was selected for subsequent electroporation experiments.

Distribution and persistence of fluorescent protein expression following electroporation

Although optimized electroporation conditions increased the proportion of GFP-positive cells to approximately 40%, fluorescence intensity remained low across transfected animals. We hypothesized that this weak signal likely reflects inherently low abundance of transcribed mRNA in *T. adhaerens*, potentially due to small cell size (3–5 μm) and compact genome (98 Mb), which may constrain transcription and translation efficiency. To further investigate this possibility, immunofluorescence staining with a GFP antibody was performed to enhance signal detection. Following staining, widespread GFP signals were observed throughout the body, with notably stronger fluorescence in peripheral regions compared to central areas (Figure 2E).

The persistence of GFP expression was subsequently evaluated at both the protein and mRNA levels. As genomic integration of the plasmid is unlikely, the transgene was gradually diluted through cell divisions. Consistent with this, GFP protein signals persisted for approximately 5 days, with sparse fluorescence remaining in peripheral regions at day 5 post-transfection (Figure 2F). RT-PCR confirmed this temporal decline of GFP mRNA levels (Figure 2G). These findings indicate that electroporation supports transient transgene expression in *T. adhaerens*, with detectable signals maintained for several days following transfection.

Evaluation of the *T. adhaerens β-actin* promoter as an alternative ubiquitous regulatory element

Given the phylogenetic position of *T. adhaerens*, the CMV promoter may exhibit reduced efficiency in driving GFP expression in this basal metazoan. To improve transgene expression, endogenous promoter candidates were assessed, with a focus on *β-actin*, a commonly employed constitutive promoter in diverse animal systems. Two *β-actin* homologs were identified in the *T. adhaerens* genome (Srivastava et al., 2008) (Figure 3A). Comparative analysis of transcriptomic datasets (Eitel et al., 2018; Jin et al., 2024; Kamm et al., 2018; Najle et al., 2023) indicated that *Tad56111* displayed the highest expression among them (Figure 3B). Single-cell transcriptomic profiling further revealed broad expression of *Tad56111* across multiple cell types, with pronounced enrichment in epithelial and peptidergic populations (Figure 3C).

The promoter region upstream of *Tad56111*—extending from the stop codon of the preceding gene to the translation start site—was cloned and used to construct GFP expression vectors (Supplementary Table S1). Electroporation of these constructs resulted in fluorescence in approximately 40% of cells at 24 h post-transfection, slightly exceeding that achieved with the CMV promoter (Figure 3D). Additionally, GFP mRNA persisted for more than 6 days following transfection (Figure 3E), and immunofluorescence analysis confirmed widespread expression throughout the body (Figure 3F).

Dissection and single-cell imaging further identified GFP signals in multiple cell types, including epithelial, fiber, and diverse peptidergic cells (Figure 3G). These results demonstrate that the endogenous β-actin promoter from *Tad56111* supports broad and efficient transgene expression in *T. adhaerens*, outperforming the CMV promoter in both intensity and expression coverage.

Transgenic expression of puromycin N-acetyltransferase (*PAC*) enhances puromycin resistance in *T. adhaerens*

To further assess the effectiveness of the transgenic approach, drug resistance assays were performed in *T. adhaerens* using commonly applied antibiotics, including neomycin and puromycin. Puromycin exposure markedly suppressed growth and viability, causing complete lethality within 24 h at 5 μg/mL and inducing rounded morphology by 24 h at 4 μg/mL followed by death by 96 h (Figure 4A).

Next, to assess functional transgene expression, the *PAC* gene was introduced under the control of either the CMV or *β-actin* promoter. Starting at 24 h post-electroporation (dpe), transfected animals were treated with 3 μg/mL puromycin for three consecutive days, followed by alternating daily exposure to puromycin at 4 μg/mL and 1 μg/mL. Interestingly, at 6 dpe, puromycin treatment was associated with higher *PAC* expression relative to untreated controls, consistent with selective elimination of cells lacking the *PAC* transgene (Supplementary Figure S4). In control groups, progressive reduction in body size was evident from 4 dpe, followed by spherical morphology at 8 dpe, tissue darkening, and complete mortality by 15 dpe (Figure 4B). In contrast, transfected groups retained normal morphology through day 13 and survived up to 23 dpe under continued puromycin exposure in both CMV- and *β-actin*-driven conditions (Figure 4C). Animals expressing *PAC* under the *β-actin* promoter showed more stable body size and sustained feeding activity during the early period between 13 and 20 dpe (Figure 4B). Collectively, these results confirm that both the CMV and *β-actin* promoters effectively drive *PAC* expression and support the use of puromycin selection in *T. adhaerens*.

DISCUSSION

The phylogenetic position of placozoans as one of the earliest-diverging metazoan lineages presents a unique opportunity to investigate the molecular foundations of multicellularity. However, their asexual reproductive mode, characterized by the partitioning of thousands of somatic cells, poses a significant challenge for generating transgenic animals using conventional methods such as zygotic microinjection. Although previous studies have reported the presence of fertilized eggs and early embryos in placozoans, their existence has yet to be independently confirmed (Eitel et al., 2011). In this context, the present study established an electroporation-based strategy for transient transgene delivery in *T. adhaerens*, enabling the ectopic expression of fluorescent reporters across multiple cell types under a broadly active promoter. Despite successful expression, fluorescence intensity remained low, likely due to limited cellular volume and reduced protein synthesis. To improve promoter efficiency, an endogenous *β-actin* promoter was cloned and used as an alternative driver of gene expression, shown to enhance both expression levels and spatial coverage. These results suggest that cell-type-specific promoters should be explored in future studies to enable functional investigation of lineage-specific genes.

While the electroporation protocol provides a feasible platform for transient transgene expression, key limitations persist. The proportion of GFP-positive cells remained below 50%, and reporter expression was transient, typically declining within 6 days. Although puromycin resistance was enhanced

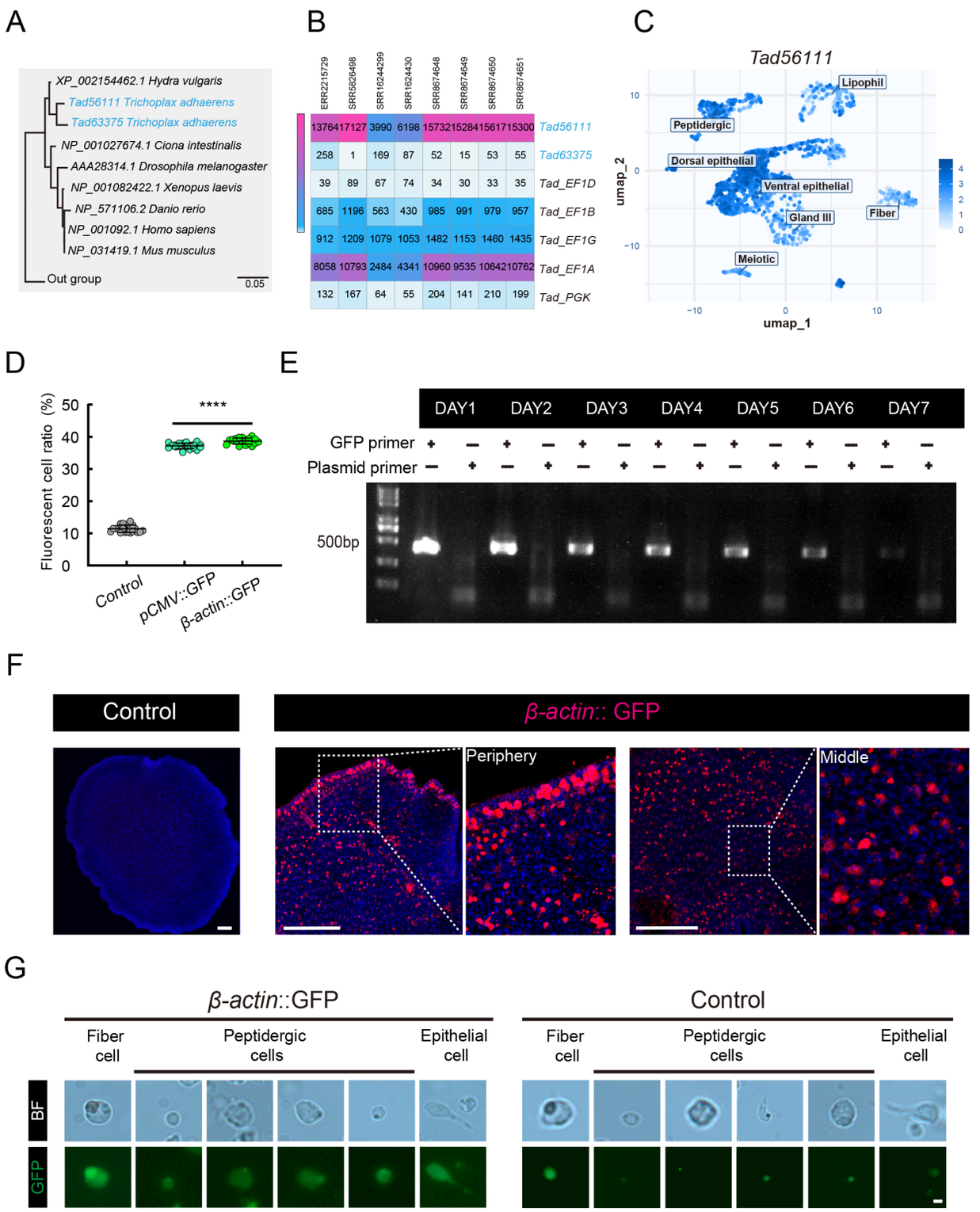

Figure 3 *β-actin* promoter-driven transgene expression in *Trichoplax adhaerens*

A: Phylogenetic analysis of metazoan *β-actin* genes constructed using the maximum-likelihood (ML) method with 1 000 bootstrap replicates. B: Heatmap showing transcriptome-based expression levels of selected housekeeping genes in *T. adhaerens*, including *Tad_EF1D* (XM_002108996.1), *Tad_EF1B* (XM_002116439.1), *Tad_EF1G* (XM_002109032.1), *Tad_EF1A* (XM_002117046.1), and *Tad_PGK* (XM_002112262.1). C: UMAP projection of single-cell transcriptomic data highlighting *Tad56111* expression across cell populations. D: Quantification of transfection efficiency based on the percentage of GFP-positive cells following electroporation. Data are presented as mean±SD. Statistical analysis was performed using unpaired Mann-Whitney tests. E: RT-PCR analysis of GFP transcript levels at multiple time points following electroporation. F: Confocal imaging of GFP expression detected via antibody staining, showing strong GFP-positive cells across both the peripheral and middle regions but weaker GFP signals in the central area. Middle region (enlarged) was imaged using higher laser power to visualize weaker GFP-expressing cells. G: GFP expression across multiple cell types under the control of the *β-actin* promoter. Scale bars: 100 μm in F and 5 μm in G. ns: Not significant; *: P<0.05; **: P<0.01; ***: P<0.001; ****: P<0.0001.

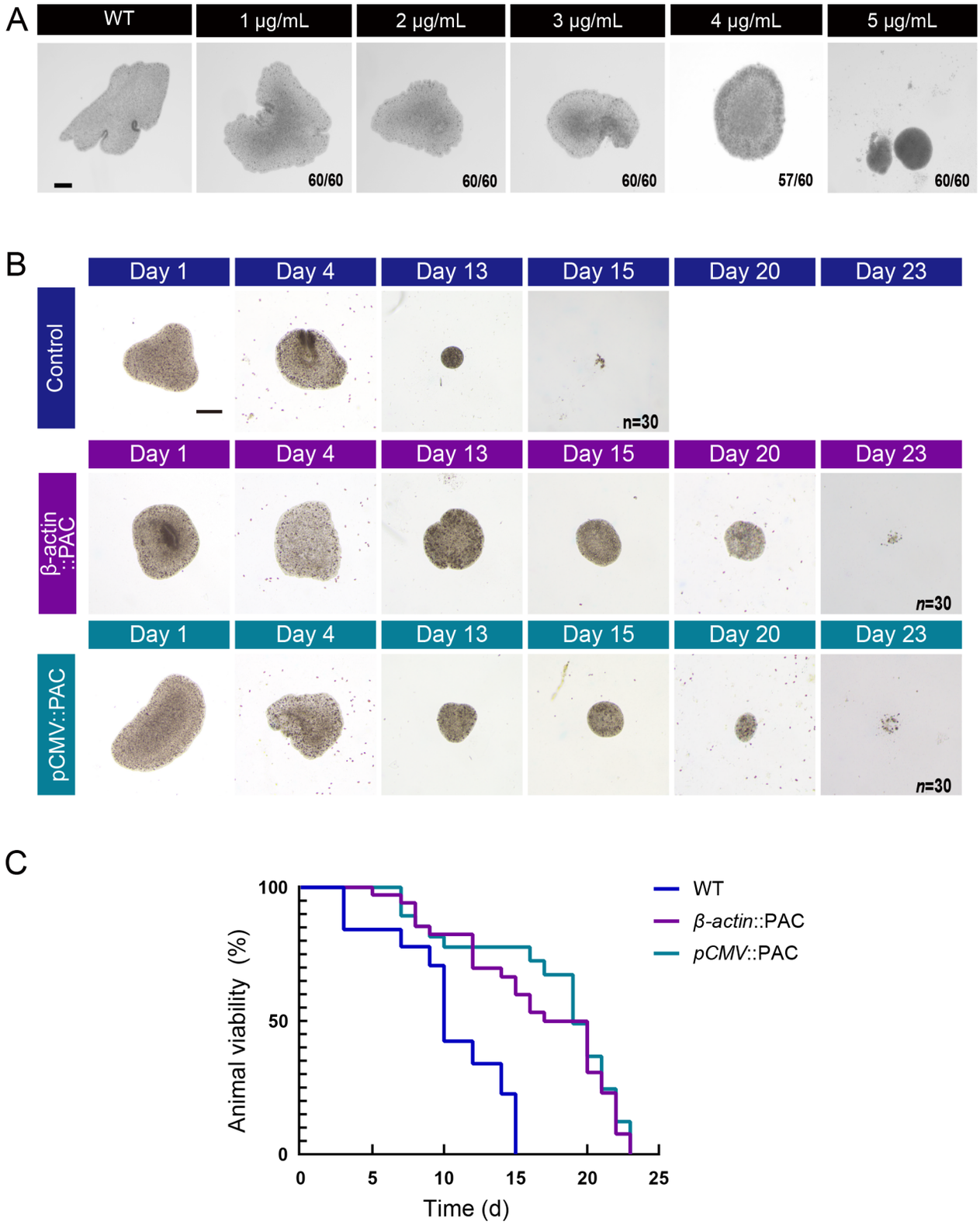

Figure 4 *PAC* expression confers puromycin resistance in *Trichoplax adhaerens*

A: External morphology of *T. adhaerens* following 24 h of exposure to increasing concentrations of puromycin. Numbers below each image indicate the number of animals examined. Higher concentrations induced spherical morphology, progressive darkening, and tissue disintegration. B: Morphological comparison of animals treated with puromycin at various time points post-electroporation in control, *β-actin*::*PAC*, and *pCMV*::*PAC* groups. C: Survival curves comparing control, *β-actin*::*PAC*, and *pCMV*::*PAC* groups following puromycin treatment. Scale bars: 100 μm in B.

in animals expressing *PAC*, long-term viability was not sustained. Establishing stable transgenic lines remains essential for long-term functional studies in *T. adhaerens,* but achieving this requires genomic integration of the reporter gene. In mammalian systems, lentiviral and adenoviral vectors are routinely used for stable genomic insertion, yet no endogenous or engineered viruses are currently known to infect placozoans. Transposon-based strategies have proven

effective in numerous model organisms (Koichi Kawakami et al., 1998), but the T. adhaerens genome contains very few active transposable elements (Shi Wang, 2010), limiting the utility of this approach. Alternatively, non-viral methods such as restriction enzyme–mediated insertion (REMI), as successfully applied in *Xenopus laevis*, and meganuclease-mediated insertion, as demonstrated in *Nematostella vectensis* through the stable generation of transgenic lines via zygotic injection of I-SceI meganuclease, offer potential routes for genomic incorporation (Ogino et al., 2006; Renfer & Technau, 2017).

Therefore, co-transfection of meganuclease-expressing plasmids alongside reporter constructs may promote genomic integration in *T. adhaerens*. Incorporation of selection markers such as puromycin resistance may further improve recovery and maintenance of stable transgenic lines.

The establishment of functional genetic tools in *T. adhaerens* represents a critical advance for placozoan research and more broadly for evolutionary developmental biology. Transgenesis, in combination with targeted gene knockdown or knockout techniques, will provide a molecular framework for studying gene regulatory networks, cellular differentiation programs, and ancestral developmental mechanisms. This work provides the foundation for experimental manipulation in *T. adhaerens* and opens new avenues for exploring the genomic and cellular innovations that underpin early animal evolution.

SUPPLEMENTARY DATA

Supplementary data to this article can be found online.

COMPETING INTERESTS

The authors declare that they have no competing interests.

AUTHORS' CONTRIBUTIONS

C.T.Z. and M.J.J. designed the research; M.J.J., Z.Y.J., Z.Y.Z., Q.Y.G., and G.T.D. performed the research; M.J.J., Z.Y.J., Z.Y.Z., Q.Y.G., and W.Q.L. analyzed the data; C.T.Z. and M.J.J. wrote the paper. All authors read and approved the final version of the manuscript.

ACKNOWLEDGMENTS

The *Trichoplax adhaerens* strain was a kind gift from Drs. Leo Buss (Yale University) and Carolyn L. Smith (National Institutes of Health). We thank members of the Zhao Lab and Fang Center for their kind help during the preparation of this manuscript. We also gratefully acknowledge the outstanding support from the core facilities of the IEMB and FANG Center at the Ocean University of China.

REFERENCES

Bi X-P & Zhang G-J. 2021. Ancestral developmental potentials in early bony fish contributed to vertebrate water-to-land transition. *Zoological Research*, **42**(2): 135–137.

Christiaen L, Wagner E, Shi WY, et al. 2009. Electroporation of transgenic DNAs in the sea squirt Ciona. *Cold Spring Harbor Protocols*, **2009**(12): pdb. prot5345.

Eitel M, Guidi L, Hadrys H, et al. 2011. New insights into placozoan sexual reproduction and development. *PLoS One*, **6**(5): e19639.

Eitel M, Francis WR, Varoqueaux F, et al. 2018. Comparative genomics and the nature of placozoan species. *PLoS Biology*, **16**(7): e2005359.

Fu JY, Han WW, Zhang X, et al. 2022. Silica nanoparticles with virus-mimetic spikes enable efficient siRNA delivery in vitro and in vivo. *Research*, **2022**: 0014.

Heyland A, Croll R, Goodall S, et al. 2014. *Trichoplax adhaerens*, an enigmatic basal metazoan with potential. *In*: Carroll DJ, Stricker SA. Developmental Biology of the Sea Urchin and Other Marine Invertebrates. Totowa: Humana Press, 45–61.

Jackson AM, Buss LW. 2009. Shiny spheres of placozoans (*Trichoplax*) function in anti‐predator defense. *Invertebrate Biology*, **128**(3): 205–212.

Jin MJ, Li WQ, Ji ZY, et al. 2024. Coordinated cellular behavior regulated by epinephrine neurotransmitters in the nerveless placozoa. *Nature Communications*, **15**(1): 8626.

Kamm K, Osigus HJ, Stadler PF, et al. 2018. *Trichoplax* genomes reveal profound admixture and suggest stable wild populations without bisexual reproduction. *Scientific Reports*, **8**(1): 11168.

Kawakami K, Koga A, Hori H, et al. 1998. Excision of the *Tol2* transposable element of the medaka fish, *Oryzias latipes*, in zebrafish, *Danio rerio*. *Gene*, **225**(1-2): 17–22.

Mayorova TD, Hammar K, Jung JH, et al. 2021. Placozoan fiber cells: mediators of innate immunity and participants in wound healing. *Scientific Reports*, **11**(1): 23343.

Najle SR, Grau-Bové X, Elek A, et al. 2023. Stepwise emergence of the neuronal gene expression program in early animal evolution. *Cell*, **186**(21): 4676–4693. e29.

Ogino H, McConnell WB, Grainger RM. 2006. High-throughput transgenesis in *Xenopus* using *I-SceI* meganuclease. *Nature Protocols*, **1**(4): 1703–1710.

Renfer E, Technau U. 2017. Meganuclease-assisted generation of stable transgenics in the sea anemone *Nematostella vectensis*. *Nature Protocols*, **12**(9): 1844–1854.

Schierwater B, Osigus HJ, Bergmann T, et al. 2021. The enigmatic Placozoa part 1: exploring evolutionary controversies and poor ecological knowledge. *Bioessays*, **43**(10): 2100080.

Schultz DT, Haddock SHD, Bredeson JV, et al. 2023. Ancient gene linkages support ctenophores as sister to other animals. *Nature*, **618**(7963): 110–117.

Schulze FE. 1883. Trichoplax adhaerens, nov. gen. , nov. spec. *Zoologischen Anzeiger*, **6**: 92–97.

Smith CL, Mayorova TD. 2019. Insights into the evolution of digestive systems from studies of *Trichoplax adhaerens*. *Cell and Tissue Research*, **377**(3): 353–367.

Smith CL, Pivovarova N, Reese TS. 2015. Coordinated feeding behavior in *Trichoplax*, an animal without synapses. *PLoS One*, **10**(9): e0136098.

Smith CL, Reese TS. 2016. Adherens junctions modulate diffusion between epithelial cells in *Trichoplax adhaerens*. *The Biological Bulletin*, **231**(3): 216–224.

Srivastava M, Begovic E, Chapman J, et al. 2008. The *Trichoplax* genome and the nature of placozoans. *Nature*, **454**(7207): 955–960.

Varoqueaux F, Williams EA, Grandemange S, et al. 2018. High cell diversity and complex peptidergic signaling underlie placozoan behavior. *Current Biology*, **28**(21): 3495–3501. e2.

Wang S, Zhang LL, Meyer E, et al. 2010. Genome-wide analysis of transposable elements and tandem repeats in the compact placozoan genome. *Biology Direct*, **5**: 18.